DALTON
FULL PAPER

Ruthenium mononitro and mononitroso terpyridine complexes incorporating azoimine based ancillary ligands. Synthesis, crystal structure, spectroelectrochemical properties and kinetic aspects †

Biplab Mondal,[a] Himadri Paul,[a] Vedavati G. Puranik[b] and Goutam Kumar Lahiri *[a]

[a] *Department of Chemistry, Indian Institute of Technology, Bombay, Mumbai-400076, India*
[b] *Physical Chemistry Division, National Chemical Laboratory, Pune, Maharashtra-411008, India*

Received 3rd October 2000, Accepted 28th November 2000
First published as an Advance Article on the web 24th January 2001

Ruthenium mononitro and mononitroso terpyridine complexes incorporating strong π-acidic azopyridine ligands of the types $[Ru^{II}(trpy)(L)(NO_2)]ClO_4$ **6**–**10** and $[Ru^{II}(trpy)(L)(NO)][ClO_4]_3$ **11**–**15** [trpy = 2,2′ : 6′,2″-terpyridine; L = $NC_5H_4N{=}NC_6H_4(R)$, R = H, *m*-Me/Cl or *p*-Me/Cl] respectively have been synthesized starting from $[Ru^{II}(trpy)L(H_2O)]^{2+}$ **1**–**5**. The single crystal X-ray structure of the nitro complex **7** has been determined. In acetonitrile solvent the nitro complexes exhibit strong MLCT transitions near 500 nm and the same MLCT bands are observed to be blue shifted near 370 nm in the case of the nitroso derivatives. The nitrosyl complexes exhibit ν_{NO} in the range 1960–1950 cm^{-1}. The nitro (**6**–**10**) and nitroso (**11**–**15**) complexes exhibit ruthenium(II)–ruthenium(III) oxidation in the ranges 1.33–1.47 V and 1.62–1.72 V *versus* SCE respectively. The nitroso complexes exhibit two successive one-electron reductions near 0.7 and 0.0 V due to reductions of coordinated $NO^+ \longrightarrow NO$ and $NO \longrightarrow NO^-$ respectively. All the complexes (**6**–**15**) systematically display three ligand based (trpy and L) reductions to negative potentials of the SCE. The nitro complexes (**6**–**10**) display weak emissions near 700 nm ($\Phi = 0.83 \times 10^{-2}$–$2.98 \times 10^{-2}$). The electrochemically generated $\mathbf{6}^+$–$\mathbf{10}^+$ show LMCT transitions near 490 nm and rhombic EPR spectra in acetonitrile at 77 K. The pseudo first order rate constants (k) and the thermodynamic parameters ($\Delta H^{\ddagger}$, $\Delta S^{\ddagger}$ and K) for formation of the nitro complexes, $[Ru^{II}(trpy)(L)(H_2O)]^{2+} \longrightarrow [Ru^{II}(trpy)(L)(NO_2)]^+$, and the conversion $[Ru^{II}(trpy)(L)(NO)]^{3+} \longrightarrow [Ru^{II}(trpy)(L)(NO_2)]^+$ have been determined.

Introduction

The recent observations of the relevance of nitric oxide (NO) in a wide range of biological and environmental processes have led to a resurgence of interest in the area of nitrosyl chemistry.[1] Moreover, the development of metal nitrosyl complexes having a high degree of electrophilic character of the coordinated NO function ($\nu_{NO} > 1900$ cm^{-1}) is a formidable challenge, since the electrophilic NO^+ centre is susceptible to fascinating molecular transformations in contact with nucleophiles.[2]

Extensive studies have been made on ruthenium nitrosyls and appreciable variation of the electronic aspect of the NO function attached to the metal centre has been observed depending on the nature of the ancillary groups present.[3] This has prompted us to develop a new class of ruthenium nitrosyl complexes encompassing a combination of strong π-acidic heterochelates. The primary intention is to introduce a high degree of electrophilicity at the nitrosyl centre and subsequently explore the reactivity of this centre to nucleophiles. A new class of ruthenium nitrosyl complexes of the type $[Ru^{II}(trpy)(L)(NO)]^{3+}$ (trpy = 2,2′ : 6′,2″-terpyridine; L = azo-imine functionalities) and their precursor nitro complexes $[Ru^{II}(trpy)(L)(NO_2)]^+$ have been synthesized. The azopyridine ligand (L) has selectively been chosen as this in combination with terpyridine has generated highly acidic aqua derivatives.[4] Consequently the presesent nitrosyl derivatives $[Ru^{II}(trpy)(L)(NO)]^{3+}$ exhibit the strongest electrophilic NO centre ($\nu_{NO} \approx 1960$ cm^{-1}) ever reported in ruthenium mononitrosyl chemistry. Herein we report the synthesis, spectroelectrochemical properties, kinetic and thermodynamic aspects of the nitrosyl as well as their precursor nitro complexes and the crystal structure of a representative nitro-derivative.

† Electronic supplementary information (ESI) available: microanalytical, IR and conductivity data for **6**–**15**; rate constants and activation parameters for **1**–**5** ⟶ **6**–**10**; time evolution of the electronic spectrum of complex **3**. See http://www.rsc.org/suppdata/dt/b0/b007975h/

Results and discussion

Synthesis

The precursor nitro complexes $[Ru^{II}(trpy)(L^{1\text{–}5})(NO_2)]^+$ **6**–**10** have been synthesized from the corresponding aqua derivatives $[Ru^{II}(trpy)(L^{1\text{–}5})(H_2O)]^{2+}$ **1**–**5** in the presence of an excess of sodium nitrite (Scheme 1). The pure complexes have been

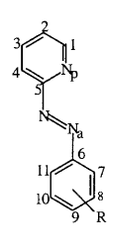

$[Ru^{II}(trpy)(L^{1\cdot 5})(H_2O)]^{2+} \xrightarrow{(i)} [Ru^{II}(trpy)(L^{1\cdot 5})(NO_2)]^+$

	R		
L^1	H	**1**	**6**
L^2	8-Me	**2**	**7**
L^3	8-Cl	**3**	**8**
L^4	9-Me	**4**	**9**
L^5	9-Cl	**5**	**10**

Scheme 1 (i) $NaNO_2$, water, Δ.

DOI: 10.1039/b007975h

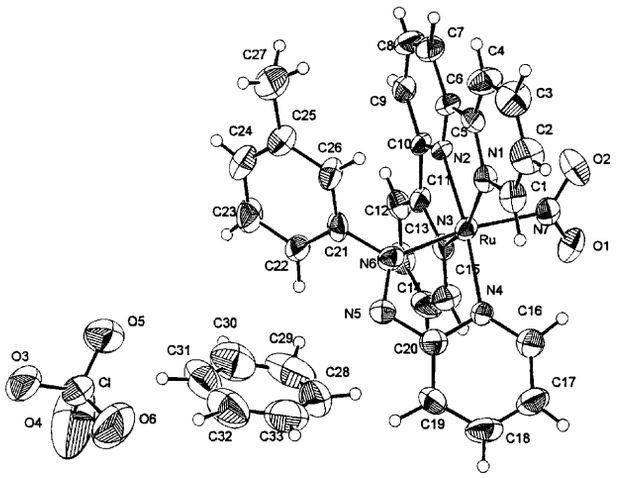

Fig. 1 An ORTEP diagram of $[Ru^{II}(trpy)(L^2)(NO_2)]ClO_4 \cdot C_6H_6$ **7**.

isolated as their perchlorate salts, $[Ru^{II}(trpy)(L^{1-5})(NO_2)][ClO_4]$. The crystal structure of a representative nitro compound (**7**) has been determined (see later) and it shows that the geometry of the starting aqua complex (N_a *trans* to H_2O) (which has been established earlier[4]) is retained in the nitro species (N_a *trans* to NO_2). Since the spectral and electrochemical properties of **7** are akin to those of the other nitro complexes, it may logically be considered that all the complexes **6**–**10** have the same geometry.

The nitroso complexes $[Ru^{II}(trpy)(L^{1-5})(NO)]^{3+}$ **11**–**15** have been made from the corresponding solid nitro derivatives **6**–**10** by using concentrated nitric acid followed by concentrated perchloric acid at 273 K. The nitro ⟶ nitroso conversion does not take place in dilute aqueous acidic media. The tricationic yellow nitroso complexes **11**–**15** have been isolated as their perchlorate salts. Since the reaction of H^+ with the peripheral NO_2 group is the primary step in the nitrosation reaction it can be assumed that the geometry of the precursor nitro complexes **6**–**10** remains unaltered in **11**–**15**.

The nitro complexes **6**–**10** are stable enough both in the solid and solution states, whereas nitroso complexes **11**–**15** are stable only in the solid state. In solution they convert back into the nitro state spontaneously in the presence of a slight amount of moisture. Therefore, the solution studies related to nitroso complexes have been performed specifically only in HPLC grade dry solvents and with minimum exposure of air.

Complexes **6**–**15** are diamagnetic at 298 K and exhibit satisfactory microanalytical and conductivity data (ESI supplementary Table 1).

Crystal structure of $[Ru^{II}(trpy)(L^2)(NO_2)]ClO_4 \cdot C_6H_6$ 7

The crystal structure of the complex $[Ru(trpy)(L^2)NO_2]ClO_4$ **7** is shown in Fig. 1 and selected bond lengths and angles are listed in Table 1. The crystal contains an array of $[Ru^{II}(trpy)(L^2)(NO_2)]^+$ cations, ClO_4^- anions and benzenes of crystallisation in a 1 : 1 : 1 stoichiometry. The terpyridine ligand is coordinated in the expected meridional fashion with the ligand L^2 in *cis* orientation.[6] The NO_2^- group is *trans* to the azo nitrogen (N_a) of L^2. The geometrical constraints imposed on the meridional terpyridine ligand are reflected in the *trans* angle, N(1)–Ru–N(3), 158.1(2)°.[7] The Ru–N(2) distance [1.971(5) Å] (central pyridyl group of terpyridine) is approximately 0.1 Å shorter than the terminal Ru–N bonds [Ru–N(1), 2.067(5) and Ru–N(3), 2.076(5) Å]. To optimise the chelation of terpyridine, the central Ru–N bond shortens while the terminal lengthen, which maintains a typical trpy bite angle of ≈7 9°.[4,6,7]

The ligand L^2 is bound to the ruthenium ion with the pyridine nitrogen (N_p) and the azo nitrogen (N_a) having a bite angle of 75.6(2)°. The shorter Ru–N(6) (azo) distance, 1.989(6) Å, compared to Ru–N(4)(pyridine), 2.057(5) Å, is due to strong $(d\pi)Ru^{II} \longrightarrow \pi^*$(azo) back bonding.[8]

Table 1 Selected bond distances (Å) and angles (°) and their standard deviations for $[Ru(trpy)(L^2)NO_2]ClO_4 \cdot C_6H_6$

Ru–N(1)	2.067(5)	Ru–N(7)	2.057(6)
Ru–N(2)	1.971(5)	N(5)–N(6)	1.274(7)
Ru–N(3)	2.076(5)	N(7)–O(1)	1.261(7)
Ru–N(4)	2.057(5)	N(7)–O(2)	1.230(7)
Ru–N(6)	1.989(6)	—	—
N(6)–Ru–N(2)	98.1(2)	N(1)–Ru–N(3)	158.1(2)
N(6)–Ru–N(4)	75.6(2)	N(6)–Ru–N(7)	171.3(2)
N(2)–Ru–N(4)	173.4(2)	N(2)–Ru–N(7)	90.0(2)
N(6)–Ru–N(1)	97.2(2)	N(4)–Ru–N(7)	96.1(2)
N(2)–Ru–N(1)	78.9(2)	N(1)–Ru–N(7)	87.3(2)
N(4)–Ru–N(1)	103.8(2)	N(3)–Ru–N(7)	88.6(2)
N(6)–Ru–N(3)	89.8(2)	Ru–N(7)–O(1)	119.7(5)
N(2)–Ru–N(3)	79.6(2)	Ru–N(7)–O(2)	122.7(5)
N(4)–Ru–N(3)	98.0(2)	O(1)–N(7)–O(2)	117.6(6)

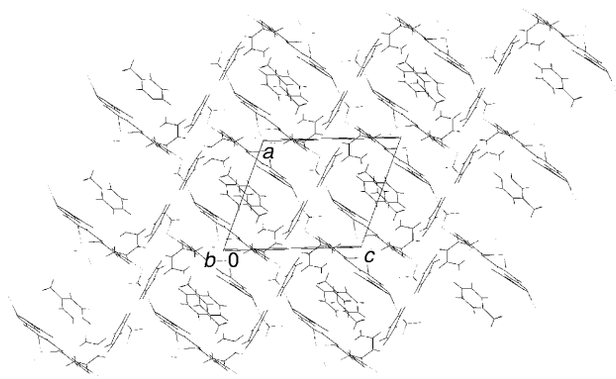

Fig. 2 Packing diagram of $[Ru^{II}(trpy)(L^2)(NO_2)]ClO_4 \cdot C_6H_6$ **7** (down *b* axis).

In complex **7** the nitrite ligand is linked to the ruthenium centre through the nitrogen atom.[9,10] The Ru–N(7)(nitro) bond distance of 2.057(6) Å is shorter than that reported for other nitroruthenium(II) complexes, such as 2.074(6) and 2.078(3), 2.080(3) Å for $[Ru^{II}(NO_2)(PMe_3)_2(trpy)]ClO_4$[11] and $Na_2[Ru(NO_2)_4(NO)(OH)]$[12] respectively. The presence of the strong π acceptor N=N function which is *trans* to the NO_2 group in **7** possibly strengthens the M–NO_2 interaction. The two N–O bond distances for the nitro ligand are 1.261(7) [N(7)–O(1)] and 1.230(7) Å [[N(7)–O(2)]. The O(1)–N(7)–O(2) angle is found to be 117.6(6)° which falls in the range 113–127° observed in other transition metal nitro complexes.[9,13] The two Ru–N–O angles are very similar, Ru–N(7)–O(1), 119.7(5) and Ru–N(7)–O(2), 122.7(5)°.

The packing diagram of the molecule (viewed down the *b* axis) is shown in Fig. 2. It can be seen that the arrays of $[Ru^{II}(trpy)(L^2)(NO_2)]^+$ cations are packed almost perpendicular to the ClO_4^- anions along with benzene molecules of crystallisation. The crystal structure is stabilised by a number of intra- and inter-molecular hydrogen bonds.

To the best of our knowledge, this work demonstrates the first crystal structure of a nitro-derivative of ruthenium terpyridine as well as ruthenium azopyridine complex systems.

Spectral aspects

Selected IR frequencies are listed in ESI supplementary Table 1. The three notable features are: (i) the N=N stretching frequency of coordinated L (≈1300 cm^{-1}) has been reasonably lowered as compared to that of free L (≈1425 cm^{-1}) due to $d\pi\ Ru^{II} \longrightarrow \pi^*$(L) back bonding;[14] (ii) the NO_2 stretching frequency for complexes **6**–**10** appears near 1350 cm^{-1};[15] (iii) one strong and sharp band has been observed consistently in the range 1960–1950 cm^{-1} for the nitroso complexes which is conspicuously

Table 2 Electronic[a] and emission[b] spectral data

Compound	UV/VIS λ/nm (ε/dm^3 mol^{-1} cm^{-1})	λ_{max}/nm (emission)	Quantum yield (Φ)
6	507 (9270), 309 (28320), 289 (23190), 274 (22360), 222 (56716)	695	0.92×10^{-2}
7	510 (11890), 328 (28390), 312 (30240), 270 (30140), 210 (58482)	702	1.25×10^{-2}
8	510 (8930), 382 (23520), 307 (24390), 272 (23830), 212 (46634)	723	0.83×10^{-2}
9	514 (8290), 329 (20280), 314 (20650), 270 (21600), 205 (44824)	707	2.98×10^{-2}
10	512 (8190), 328 (21020), 310 (18320), 271 (22940), 209 (46178)	717	1.81×10^{-2}
11	366 (8540), 326 (10980), 289 (12510), 228 (29960)	—	—
12	365 (12100), 328 (15970), 289 (18330), 228 (47690)	—	—
13	368 (7520), 329 (9040), 291 (10700), 230 (26920)	—	—
14	371 (9653), 332 (13160), 292 (14420), 230 (39991)	—	—
15	369 (9450), 328 (11300), 290 (10120), 230 (25490)	—	—
$\mathbf{6}^+$	495 (6450), 370 (7200), 328 (11800), 312 (19490), 281 (18290)	—	—
$\mathbf{7}^+$	488 (7040), 365 (5310), 329 (17130), 314 (15750), 284 (18860)	—	—
$\mathbf{8}^+$	492 (6810), 371 (4460), 328 (18120), 313 (16400), 283 (18580)	—	—
$\mathbf{9}^+$	490 (6970), 370 (6650), 328 (17510), 314 (15500), 284 (19170)	—	—
$\mathbf{10}^+$	494 (5840), 366 (7200), 329 (15620), 313 (15520), 282 (16100)	—	—

[a] In acetonitrile at 298 K. [b] In ethanol–methanol (4 : 1 v/v) at 77 K.

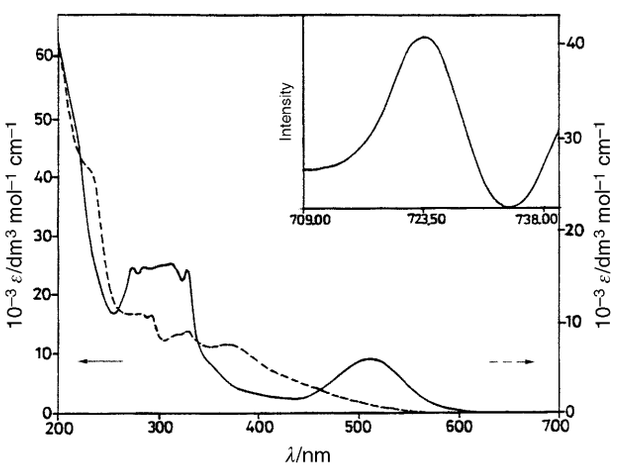

Fig. 3 Electronic spectra of $[Ru^{II}(trpy)(L^3)(NO_2)]ClO_4$ **8** (——) and $[Ru^{II}(trpy)(L^3)(NO)][ClO_4]_3$ **13** (- - - -) in dry acetonitrile. Inset shows the emission spectrum of **8** in EtOH–MeOH 4 : 1 (v/v) at 77 K.

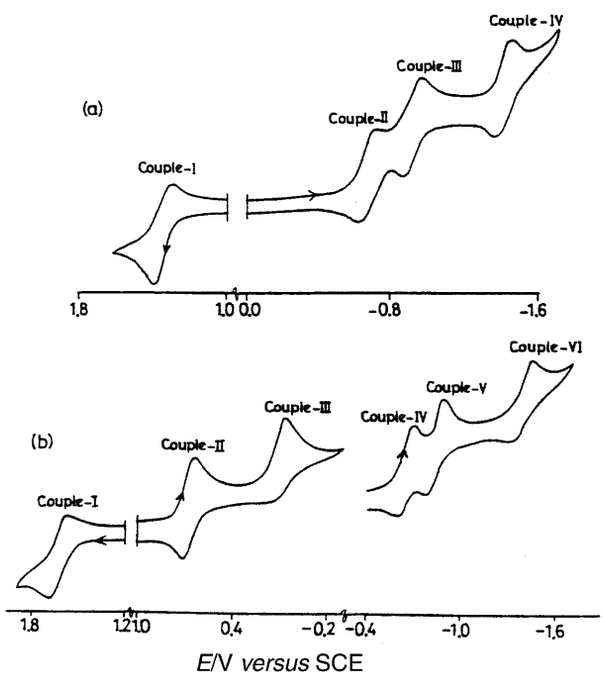

Fig. 4 Cyclic voltammograms of $\approx 10^{-3}$ mol dm^{-3} solutions of the complexes (a) $[Ru^{II}(trpy)(L^2)(NO_2)]ClO_4$ **7** and (b) $[Ru^{II}(trpy)(L^2)(NO)][ClO_4]_3$ **12** in dry acetonitrile.

absent in the spectra of the precursor nitro complexes **6**–**10**. This is evidently due to the stretching mode of ν(NO) of the coordinated nitrosyl group.[16] Such a high ν(NO) frequency implies that formally a linear NO^+ unit is linked to the metal centre.[17] It may be noted that the present set of nitrosyl complexes **11**–**15** exhibit the highest ν(NO) frequency so far observed in ruthenium mononitrosyl complexes. This is possibly due to the serious electronic impact of the strong π-acidic azopyridine ligand (L) in combination with the terpyridyl group on the nitrosyl function.

In acetonitrile solvent the complexes exhibit multiple transitions in the UV-Visible region (Table 2, Fig. 3). The nitro complexes **6**–**10** display the lowest energy MLCT bands near 500 nm. Their intense visible (≈500 nm) absorption bands systematically blue shifted (near 370 nm) while moving to the nitroso complexes **11**–**15** (Fig. 3, Table 2). This has been attributed to the effect of $d\pi \longrightarrow \pi^*(NO)$ back bonding, which essentially stabilises the dπ level and consequently shifts the MLCT band to the UV region.[18,19] The intra ligand (π–π* and n–π*) transitions appear in the UV region.[4]

Excitation of complexes **6**–**10** in an optically dilute MeOH–EtOH (1 : 4 v/v) rigid glass (77 K) at the lowest energy MLCT band (λ_{max} near 500 nm) results in weak emissions near 700 nm (Table 2, Fig. 3). These are believed to be originated from the ^{3}MLCT excited state.[20] The quantum yields (Φ) of the emission processes were measured in an EtOH–MeOH (4 : 1 v/v) rigid glass at 77 K relative to that of $[Ru(bpy)_3][PF_6]_2$ ($\Phi = 0.35$[21]) by following the reported procedure.[22,23] The calculated quantum yields are listed in Table 2 and show reasonable variations depending on the location and nature of the 'R' functions.

Electron-transfer properties

The reduction potential data of the complexes in acetonitrile solvent are listed in Table 3 and representative voltammograms are shown in Fig. 4. The nitro complexes **6**–**10** exhibit a quasi-reversible oxidative couple (couple I) in the range 1.35–1.47 V (Table 3, Fig. 4a). This is assigned to the ruthenium(III)–ruthenium(II) couple. Its one-electron nature is confirmed by constant-potential coulometry (Table 3). The presence of trivalent ruthenium in the oxidised solution is evidenced by the characteristic rhombic EPR spectrum of the ruthenium(III) complex.[24] The formal potential of the couple varies depending on the 'R' groups present in the framework of L (Table 3).[25] Under identical experimental conditions the ruthenium(III)–ruthenium(II) couple of the similar chloro complexes $[Ru^{II}(trpy)(L^{1-5})(Cl)]^+$ appears in the range 1.10–1.24 V *versus*

Table 3 Electrochemical data in acetonitrile at 298 K [a]

Compound	Ru^{III}–Ru^{II} couple I		Ligand reductions, E°_{298}/V (ΔE_p/mV)					
	E^{0}_{298}/V (ΔE_p/mV)	n [b]	couple II	n [b]	couple III	couple IV	couple V	couple VI
6	1.39(70)	1.05	—	—	—	−0.61(80)	−0.88(80)	−1.37(80)
7	1.35(80)	1.08	—	—	—	−0.64(70)	−0.92(90)	−1.39(70)
8	1.43(80)	0.96	—	—	—	−0.59(70)	−0.85(80)	−1.34(90)
9	1.33(70)	1.08	—	—	—	−0.67(80)	−0.94(80)	−1.44(80)
10	1.47(80)	1.05	—	—	—	−0.57(80)	−0.81(70)	−1.31(80)
11	1.72 [c]		0.72(90)	1.09	0.07 [c]	−0.60(70)	−0.85(80)	−1.38(100)
12	1.64(80)		0.69(80)	0.96	0.06 [c]	−0.65(80)	−0.85(110)	−1.40(110)
13	—		0.68(60)	0.94	0.09 [c]	−0.58(80)	−0.80(80)	−1.35(90)
14	1.62(80)		0.70(80)	0.97	0.07 [c]	−0.68(90)	−0.86(90)	−1.42(100)
15	—		0.69(80)	0.96	0.06 [c]	−0.55(80)	−0.80(80)	−1.32(100)

[a] Solvent, acetonitrile; supporting electrolyte, $[NEt_4][ClO_4]$; reference electrode, SCE; solute concentration, $\approx 10^{-3}$ mol dm^{-3}; working electrode, platinum wire. Cyclic voltammetric data: scan rate, 50 mV s^{-1}; $E^{\circ}_{298} = 0.5(E_{pa} + E_{pc})$ where E_{pa} and E_{pc} are the anodic and cathodic peak potentials, respectively. [b] $n = Q/Q'$, where Q' is the calculated coulomb count for $1e^-$ transfer and Q the coulomb count found after exhaustive electrolysis of $\approx 10^{-2}$ mol dm^{-3} solutions of the complexes. [c] E_{pa} values are considered due to the irreversible nature of the voltammograms.

SCE.[4] Therefore, the substitution of Cl^- group by the stronger electron withdrawing NO_2^- function results in an increase in metal redox potential by ≈0.2 V. The similar bipyridine complex $[Ru^{II}(trpy)(bpy)(NO_2)]^+$ displays the Ru^{III}–Ru^{II} couple at 1.05 V.[26,27] The stronger π-acidic nature of L compared to bpy is the key factor in forcing the metal redox at a higher potential for the present set of complexes.[28,29]

The nitrosyl complexes **11**–**15** display multiple redox processes in the experimental potential range (couples I–VI). At the positive side of the SCE they exhibit systematically one reversible reductive process near 0.7 V (couple II) followed by another irreversible reduction near 0.0 V (couple III) (Table 3, Fig. 4b). The one-electron stoichiometry of the reversible reductive process II is established by constant-potential coulometry (Table 3). The reduced species is found to be unstable even at 273 K, which has precluded its isolation and further studies. The one-electron nature of the other couples (I and III–VI) is confirmed by differential pulse voltammetry. The first two reductions (couples II and III) are assigned to successive one-electron reductions of the coordinated NO^+ unit, eqns. (1) and (2). This assignment is based on earlier observations of

$$[Ru^{II}(trpy)(L)(NO)]^{3+} + e^- \rightleftharpoons [Ru^{II}(trpy)(L)(NO)]^{2+} \quad (1)$$

$$[Ru^{II}(trpy)(L)(NO)]^{2+} + e^- \longrightarrow [Ru^{II}(trpy)(L)(NO)]^{+} \quad (2)$$

the similar ruthenium bipyridine system.[30] The bpy complex of similar type, $[Ru(trpy)(bpy)(NO)]^{3+}$, exhibits the two one-electron reduction processes, eqns. (1) and (2), at 0.45 and −0.20 V respectively.[30] Therefore a positive shift of ≈0.20–0.25 V of the reduction potentials of coordinated NO^+ has taken place while switching from an environment of bpy to L. This is attributed to the stronger π-acidic nature of L as compared to bpy. Moreover, the reduction potential of $Ru–NO^+ \longrightarrow Ru–NO$ [couple II, eqn. (1)] of complexes **11**–**15** is close to that of uncoordinated NO^+ ($E°$/V 0.74).[31] This reveals that the electrophilicity of the coordinated NO in the present set of complexes is comparable to that of free NO^+. The insignificant π interaction of NO in the present nitrosyl complexes **11**–**15** is presumably the primary dictating factor for the observed high reduction potential. Although the first reduction process $Ru–NO^+ \longrightarrow Ru–NO$ (couple II) is stable on the coulometric timescale, the second $Ru–NO \longrightarrow Ru–NO^-$ is unstable even on cyclic voltammetric timescale. To the best of our knowledge, the present work presents the most electrophilic nitrosyl centre in a ruthenium polypyridyl nitrosyl environment.

Nitrosyl complexes **12** and **14** incorporating L^2 and L^4 respectively show one additional quasi-reversible oxidation process near 1.60 V (couple I, Fig. 4b, Table 3) and in the case of **11** one irreversible oxidation process has been observed at 1.72 V (Table 3). The one-electron nature of couple I is confirmed by differential pulse voltammetry. The oxidation process corresponding to it may be assigned to the ruthenium(II)–ruthenium(III) oxidation as all other redox active centres in the complex moiety are only susceptible to reduction. The same ruthenium(II)–ruthenium(III) couple has not been detected for complexes **13** and **15** within the experimental potential limit (+2.0 V). The presence of the electron-withdrawing chloride group in the framework of L^3 and L^5 in **13** and **15** most likely pushes the ruthenium(II)–ruthenium(III) couple beyond the experimental potential limit.

The nitro as well as nitroso complexes **6**–**15** display three additional successive one-electron reductions to negative potentials of the SCE (couples II, III and IV for **6**–**10** and IV, V and VI for **11**–**15**, Fig. 4). The one-electron nature of the responses has been established by differential pulse voltammetry, which shows that all the reduction waves have the same height as that of the coulometrically established one-electron processes (couple I for **6**–**10** and II for **11**–**15**). Since both coordinated terpyridine and L are known to accept successively two electrons in their lowest unoccupied molecular orbitals,[32,33] the observed reductions are considered to be ligand based processes. Although there is no direct experimental evidence in favour of considering the observed reductions correspond to specific ligands, trpy and L, the first two reductions are believed to be associated with L. The reduction at the higher potential is possibly a terpyridine based process. This assumption is based on the fact that the azopyridine ligand is known to be a better π acceptor than are polypyridyl ligands.[34]

Electrochemical oxidations of complexes **6**–**10** in acetonitrile solvent at 1.5 V *versus* SCE develop unstable orange oxidised species. The oxidised complexes $\mathbf{6}^+$–$\mathbf{10}^+$ display voltammograms which are identical to those of the starting bivalent complexes **6**–**10**. They exhibit one intense LMCT transition in the visible region and intra-ligand transitions in the UV region (Table 2).[33] The EPR spectrum of one complex $\mathbf{7}^+$ has been recorded by quickly freezing the oxidised solution in liquid nitrogen and displays a rhombic spectrum ($g_1 = 2.730$, $g_2 = 2.135$ and $g_3 = 1.672$) characteristic of a distorted octahedral low-spin ruthenium(III) system.[35]

Although it has mentioned that the electrochemically generated trivalent Ru^{III}–NO_2 species $[Ru^{III}(bpy)_2(py)(NO_2)]^{2+}$ undergoes disproportionation to $[Ru^{III}(bpy)_2(py)(NO_3)]^{2+}$ and $[Ru^{II}(bpy)_2(py)(NO)]^{3+}$,[3] and $[Ru^{III}(NO_2)(PR_3)_2(trpy)]^{2+}$ decomposes to the nitroso species $[Ru^{II}(NO)(PR_3)_2(trpy)]^{3+}$,[15] we have not observed any such disproportionation or transformation on electrochemical oxidation of the present set of complexes.

Table 4 Rate constants, activation parameters and equilibrium constants for the process $[Ru(trpy)(L)(NO)]^{3+}$ **11–15** ⟶ $[Ru(trpy)(L)(NO_2)]^{+}$ **6–10** in the presence of a controlled water concentration (fifty times excess with respect to **11–15**)

Compound	$10^2\,k/s^{-1}$, 299 K	$10k/s^{-1}$, 309 K	$10k/s^{-1}$, 319 K	$\Delta H^{\ddagger}$/kJ mol^{-1}	$\Delta S^{\ddagger}$/J K^{-1} mol^{-1}	$10^{-5}\,K$
11	6.94	4.30	19.71	130.21	168.60	2.79
12	8.26	5.84	30.92	141.13	206.54	1.63
13	7.55	4.94	23.16	133.29	179.64	1.43
14	4.16	2.60	12.42	132.18	170.88	2.83
15	3.29	1.98	10.95	136.22	182.08	2.47

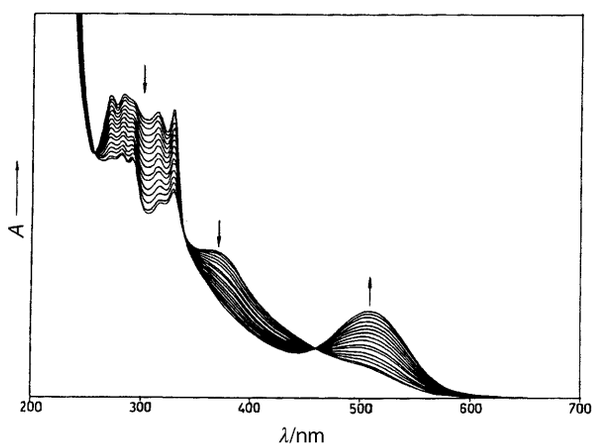

Fig. 5 Time evolution of the electronic spectra of a changing solution of $[Ru^{II}(trpy)(L^3)(NO)]^{3+}$ **13** ⟶ $[Ru^{II}(trpy)(L^3)(NO_2)]^{+}$ **8** in dry acetonitrile and in the presence of a 50 times excess of water (with respect to **13**) at 309 K. The arrows indicate increase or decrease in band intensities as the reaction proceeds.

Rate of conversion of $[Ru^{II}(trpy)(L)(H_2O)]^{2+}$ 1–5 ⟶ $[Ru^{II}(trpy)(L)(NO_2)]^{+}$ 6–10

The conversion of the aqua complexes, $[Ru^{II}(trpy)(L)(H_2O)]^{2+}$ **1–5** into the corresponding nitro species $[Ru^{II}(trpy)(L)(NO_2)]^{+}$ **6–10** has been followed spectrophotometrically in aqueous solution using an excess of aqueous $NaNO_2$ (aqua complex $NaNO_2 = 1:50$) in the temperature range 299–319 K (ESI supplementary Figure). The pseudo first order rate constants (k) and activation parameters ($\Delta H^{\ddagger}$ and $\Delta S^{\ddagger}$) are listed in ESI supplementary Table 2. Rate constant k varies systematically with respect to the electronic nature of L and follows the order **5** > **4** > **3** > **1** > **2** (ESI supplementary Table 2). The observed high enthalpy values (($\Delta H^{\ddagger}$/kJ mol^{-1}, 84.48–86.59; ESI supplementary Table 2) for the conversion process may be indicative of a dissociative process.[36] The slightly negative $\Delta S^{\ddagger}$ values ($\Delta S^{\ddagger}$/J K^{-1} mol^{-1}, −1.09 to −2.30) also suggest that the conversion process (**1–5** ⟶ **6–10**) is primarily dissociatively activated with a small contribution from the incoming ligand in the transition state.[37]

Rate of conversion of $[Ru^{II}(trpy)(L)(NO)]^{3+}$ 11–15 ⟶ $[Ru^{II}(trpy)(L)(NO_2)]^{+}$ 6–10

The present set of nitrosyl complexes are found to be stable only in dry solvent. In contact with water they spontaneously and quantitatively convert into the nitro species **6–10**. The unusually high reactivity of the nitrosyl group with water suggests a very high equilibrium constant of the conversion process in aqueous media. The presence of the strong π-acidic azopyridine ligand L *trans* to the NO function in the complexes **11–15** leads to increased electrophilicity of the coordinated nitrosyl function to a large extent which in turn facilitates the reactivity of the NO^{+} towards the nucleophile. Therefore, the rate of conversion of nitroso ⟶ nitro (eqn. (3)) has been

$$[Ru^{II}(trpy)(L)(NO)]^{3+} + H_2O \longrightarrow [Ru^{II}(trpy)(L)(NO_2)]^{+} + 2H^{+} \quad (3)$$

monitored spectrophotometrically in the temperature range 299–319 K in dry acetonitrile solvent and in the presence of a controlled concentration of water (50 times excess with respect to the complex). The well defined isosbestic points (Fig. 5) in all cases demonstrate that only the nitrosyl and nitro complexes are present in appreciable concentrations during the transition. The equilibrium constant for the conversion process (Scheme 2)

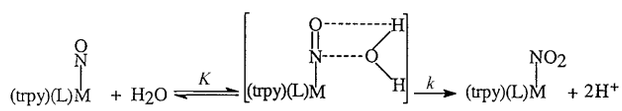

Scheme 2

has been estimated spectrophotometrically. The pseudo first order rate constants (k), the activation parameters ($\Delta H^{\ddagger}$ and $\Delta S^{\ddagger}$) and the equilibrium constant (K) values are shown in Table 4. The magnitudes of $\Delta H^{\ddagger}$ and $\Delta S^{\ddagger}$ are found to be very similar for the complexes (Table 4), implying that a similar mechanism is operative in all cases. The high positive enthalpy and entropy of activation can best be explained in terms of a dissociatively activated process as shown in Scheme 2.[36]

Conclusion

We have observed that the selective combination of a strong π-acidic azopyridine function (L) with the terpyridyl (trpy) group in the complexes $[Ru^{II}(trpy)(L)(NO)]^{3+}$ **11–15** yielded the most electrophilic nitrosyl centre in a ruthenium polypyridyl mononitrosyl environment. The present set of nitrosyl derivatives are extremely reactive even in the presence of a moist environment, spontaneously converting into the parent nitro derivatives. The detailed kinetic experiments indicate that the conversion of the nitroso, $[Ru^{II}(trpy)(L)(NO)]^{3+}$, into nitro, $[Ru^{II}(trpy)(L)(NO_2)]^{+}$, species primarily follows a dissociatively activated process. Preliminary results indicate that the nitrosyl complexes **11–15** are susceptible to fascinating reactions in the presence of a variety of nucleophiles. Further investigations in this direction are in progress.

Experimental

Materials

The starting complexes $[Ru(trpy)(L^{1-5})(H_2O)][ClO_4]_2\cdot H_2O$ **1–5**[4] and the ligands L^{1-5}[38] were prepared according to the reported procedures. 2,2′:6′,2″-Terpyridine was obtained from Aldrich, USA. Other chemicals and solvents were reagent grade and used as received. Silica gel (60–120 mesh) used for chromatography was of BDH quality. For spectroscopic and electrochemical studies HPLC grade solvents were used. Water of high purity was obtained by distillation of deionised water from $KMnO_4$. Commercial tetraethylammonium bromide was converted into pure tetraethylammonium perchlorate by following an available procedure.[39]

Physical measurements

UV-visible spectra were recorded by using a Shimadzu-2100 spectrophotometer, FT-IR spectra on a Nicolet spectro-

photometer with samples prepared as KBr pellets. Solution electrical conductivity was checked using a Systronic 305 conductivity bridge. Magnetic susceptibility was checked with a PAR vibrating sample magnetometer. Cyclic voltammetric, differential pulse voltammetric and coulometric measurements were carried out using a PAR model 273A electrochemistry system. Platinum wire working and auxiliary electrodes and an aqueous saturated calomel reference electrode (SCE) were used in a three-electrode configuration. The supporting electrolyte was $[NBu_4]ClO_4$ and the solute concentration was $\approx 10^{-3}$ mol dm^{-3}. The half-wave potential E°_{298} was set equal to $0.5(E_{pa} + E_{pc})$, where E_{pa} and E_{pc} are the anodic and cathodic cyclic voltammetric peak potentials respectively. A platinum wire-gauze working electrode was used in coulometric experiments. All experiments were carried out under a dinitrogen atmosphere and uncorrected for junction potentials. Solution emission properties were checked using a SPEX-fluorolog spectrofluorometer. The elemental analyses were carried out with a Carlo Erba (Italy) elemental analyser.

Kinetic measurements

The conversion $[Ru^{II}(trpy)(L)(H_2O)]^{2+} \longrightarrow [Ru^{II}(trpy)(L)(NO_2)]^{+}$ was monitored spectrophotometrically in thermostatted cells in the presence of an excess of $NaNO_2$ in aqueous media. The conversion $[Ru^{II}(trpy)(L)(NO)]^{3+} \longrightarrow [Ru^{II}(trpy)(L)(NO_2)]^{+}$ was monitored spectrophotometrically in thermostatted cells in a dry acetonitrile medium and in the presence of a fifty times excess of water compared to the complex concentration. For the determination of k in both cases, the increase in absorption (A_t) at 510 nm corresponding to λ_{max} of the nitro species was recorded as a function of time (t). A_α was measured when the intensity changes levelled off. Values of pseudo first order rate constants, k, were obtained from the slopes of linear least-squares plots of $\ln(A_\alpha - A_0)/(A_\alpha - A_t)$ against t. The activation parameters $\Delta H^{\ddagger}$ and $\Delta S^{\ddagger}$ were determined from the Eyring plot.[35]

Preparation of complexes

The complexes $[Ru(trpy)(L^{1\text{–}5})(NO_2)]ClO_4$ **6**–**10** were synthesized from the corresponding aqua species $[Ru(trpy)(L^{1\text{–}5})(H_2O)][ClO_4]_2 \cdot H_2O$ by following a general procedure. Yields vary in the range 80–85%. Details are given for a representative complex (**7**).

$[Ru(trpy)(L^2)(NO_2)]ClO_4$ 7. A 100 mg (0.130 mmol) quantity of $[Ru(trpy)(L^2)(H_2O)][ClO_4]_2 \cdot H_2O$ **2** was dissolved in water (20 cm^3). An excess of $NaNO_2$ (36 mg, 0.52 mmol) was added and the reaction mixture heated at reflux for 1 h. The orange solution of the starting aqua species changed to pink during the reaction. The volume of water was then reduced on a water bath (5 ml) and to it was added a saturated aqueous solution of $NaClO_4$ (3 cm^3). The crystalline pure nitro complex $[Ru(trpy)(L^2)(NO_2)]ClO_4$ **7** thus obtained was filtered off, washed with a little ice-cold water and dried *in vacuo* over P_4O_{10}. Yield: 76.90 mg (85%).

The nitroso complexes $[Ru(trpy)(L^{1\text{–}5})(NO)][ClO_4]_3$ **11**–**15** were prepared from the corresponding nitro derivatives **6**–**10** in the solid state using concentrated HNO_3–$HClO_4$. Details are mentioned for one complex **12**.

$[Ru(trpy)(L^2)(NO)][ClO_4]_3$ 12. The solid nitro complex $[Ru(trpy)(L^2)(NO_2)]ClO_4$ **7** (100 mg, 0.148 mmol) was taken in a beaker placed in an ice-bath and concentrated HNO_3 (2 cm^3) added. The mixture was made a paste by stirring with a glass rod. Ice-cold concentrated $HClO_4$ (5 cm^3) was then added dropwise with continuous stirring. A yellow solid product started developing on addition of ice-cold water and approximately 10 cm^3 water were needed to complete the precipitation. The precipitate thus obtained was filtered off immediately, washed with a little ice-cold water and dried *in vacuo* over P_4O_{10}. Yield: 0.114 mg, 90%.

Table 5 Crystallographic data for $[Ru(trpy)(L^2)(NO_2)]ClO_4 \cdot C_6H_6$ **7**

Formula	$C_{33}H_{28}ClN_7O_6Ru$
M	755.14
Crystal symmetry	Triclinic
Space group	$P\bar{1}$
a/Å	11.452(10)
b/Å	11.807(10)
c/Å	13.265(2)
α/°	82.366(9)
β/°	67.565(8)
γ/°	77.581(7)
V/Å^3	1616.5(3)
T/K	293(2)
μ/mm^{-1}	0.624
Z	2
Reflections collected	5678
Unique reflections (R_{int})	5678 (0.0000)
$R1$	0.063
$wR2$	0.106

Crystallography

Thin rectangular single crystals of complex **7** were grown by slow diffusion of an acetonitrile solution of it in benzene followed by slow evaporation. Significant crystal data and data collection parameters are listed in Table 5. The structure was solved by direct methods using SHELXS 86 and refined by full-matrix least squares on F^2 using SHELXL 97.[40] The X-ray analysis shows the presence of ClO_4^- anion and the benzene molecule as solvent of crystallisation.

CCDC reference number 186/2288.

See http://www.rsc.org/suppdata/dt/b0/b007975h/ for crystallographic files in .cif format.

Acknowledgements

Financial support received from the Department of Science and Technology, New Delhi and Council of Scientific and Industrial Research, New Delhi, India, is gratefully acknowledged. The X-ray structural studies were carried out at the National Single Crystal Diffractometer Facility, Indian Institute of Technology, Bombay. Special acknowledgement is made to Regional Sophisticated Instrumental Center, RSIC, Indian Institute of Technology, Bombay for providing the EPR facility.

References

1 K. J. Franz and S. J. Lippard, *Inorg. Chem., 2000,* **39**, 3722; M. K. Ellison, C. E. Schulz and W. R. Scheidt, *Inorg. Chem.*, 1999, **38**, 100; M. Ray, A. P. Golombek, M. C. Hendrich, G. P. A. Yap, L. M. Liable-Sands, A. L. Rheingold and A. S. Borovik, *Inorg. Chem.*, 1999, **38**, 3110; L. M. Carruthers, C. L. Closken, K. L. Link, S. N. Mahapatro, M. Bikram, J. Du, S. S. Eaton and G. R. Eaton, *Inorg. Chem.*, 1999, **38**, 3529; G. Yi, M. A. Khan, D. R. Powell and G. B. Richter-Addo, *Inorg. Chem.*, 1998, **37**, 208; M. K. Ellison and W. R. Scheidt, *Inorg. Chem.*, 1998, **37**, 382; L. Chen, M. A. Khan and G. B. Richter-Addo, *Inorg. Chem.*, 1998, **37**, 533; K. M. Miranda, X. Bu, I. Lorkovic and P. C. Ford, *Inorg. Chem.*, 1997, **36**, 4838; A. Wlodarczyk, J. P. Maher, S. Coles, D. V. Hibbs, M. H. B. Hursthouse and K. M. Abdul Malik, *J. Chem. Soc., Dalton Trans.*, 1997, 2597; P. Legzdins, S. J. Rettig, K. M. Smith, V. Tong and V. G. Young, Jr., *J. Chem. Soc., Dalton Trans.*, 1997, 3269.

2 J. A. McCleverty, *Chem. Rev.*, 1979, **79**, 53; K. K. Pandey, *Coord. Chem. Rev.*, 1983, **51**, 69; A. Das, C. J. Jones and J. A. McCleverty, *Polyhedron*, 1993, **12**, 327; D. W. Pipes and T. J. Meyer, *Inorg. Chem.*, 1984, **23**, 2466; M. H. Thiemens and W. C. Trogler, *Science*, 1991, **251**, 932; M. Feelisch and J. S. Stamler (Editors), *Methods in Nitric Oxide Research*, Wiley, Chichester, 1996.

3 D. R. Lang, J. A. Davis, L. G. F. Lopes, A. A. Ferro, L. C. G. Vasconcellos, D. W. Franco, E. Tfouni, A. Wieraszko and M. J. Clarke, *Inorg. Chem.*, 2000, **39**, 2294; B. R. McGarvey, A. A. Ferro, E. Tfouni, C. W. B. Bezerra, I. Bagatin and D. W. Franco, *Inorg.*

Chem., 2000, **39**, 3577; M. Kawano, A. Ishikawa, Y. Morioka, H. Tomizawa and E. Miki, *J. Chem. Soc.*, *Dalton Trans.*, 2000, 781; M. Kawano, A. Ishikawa, Y. Morioka, H. Tomizawa, E. Miki and Y. Ohashi, *J. Chem. Soc.*, *Dalton Trans.*, 2000, 2425; S. S. S. Broges, C. U. Davanzo, E. E. Castellano, J. Z-Schpector, S. C. Silva and D. W. Franco, *Inorg. Chem.*, 1998, **37**, 2670; P. Homanen, M. Haukka, M. Ahlgren and T. A. Pakkanen, *Inorg. Chem.*, 1997, **36**, 3794; M. R. Rhodes and T. J. Meyer, *Inorg. Chem.*, 1988, **27**, 4772; T. Uchida, R. Irie and T. Katsuki, *Tetrahedron*, 2000, **56**, 3501; A. K. Deb and S. Goswami, *Polyhedron*, 1993, **12**, 1419; F. Bottomley, W. V. F. Brooks, D. E. Paez, P. S. White and M. Mukaida, *J. Chem. Soc.*, *Dalton Trans.*, 1983, 2465; A. R. Chakravarty and A. Chakravorty, *J. Chem. Soc.*, *Dalton Trans.*, 1983, 961; W. R. Murphy, Jr., K. J. Takeuchi and T. J. Meyer, *J. Am. Chem. Soc.*, 1982, **104**, 5817; M. S. Thompson and T. J. Meyer, *J. Am. Chem. Soc.*, 1981, **103**, 5577; J. L. Walash, R. M. Bullock and T. J. Meyer, *Inorg. Chem.*, 1980, **19**, 865.

4 B. Mondal, M. G. Walawalkar and G. K. Lahiri, *J. Chem. Soc.*, *Dalton Trans.*, 2000, 4209.

5 C. K. Johnson, ORTEP II, Report ORNL-5138, Oak Ridge National Laboratory, Oak Ridge, TN, 1976.

6 A. Spek, A. Gerli and J. Reedjik, *Acta Crystallogr.*, *Sect. C*, 1994, **50**, 394; N. Grover, N. Gupta, P. Singh and H. H. Thorp, *Inorg. Chem.*, 1992, **31**, 2014.

7 B. Mondal, S. Chakraborty, P. Munshi, M. G. Walawalkar and G. K. Lahiri, *J. Chem. Soc.*, *Dalton Trans.*, 2000, 2327.

8 B. K. Santra, G. A. Thakur, P. Ghosh, A. Pramanik and G. K. Lahiri, *Inorg. Chem.*, 1996, **35**, 3050.

9 S. H. Simonsen and M. H. Mueller, *J. Inorg. Nucl. Chem.*, 1965, **27**, 309.

10 A. J. Finney, M. A. Hitchman, D. L. Kepert, C. L. Raston, G. L. Rowbottom and A. H. White, *Aust. J. Chem.*, 1981, **34**, 2177.

11 R. A. Leising, S. A. Kubow, M. R. Churchill, L. A. Buttrey, J. W. Ziller and K. J. Takeuchi, *Inorg. Chem.*, 1990, **29**, 1306.

12 E. A. Seddon and K. R. Seddon, *The Chemistry of Ruthenium*, Elsevier, New York, 1984.

13 G. R. Clark, J. M. Waters and K. R. Whittle, *J. Chem. Soc.*, *Dalton Trans.*, 1975, 2556.

14 B. K. Santra and G. K. Lahiri, *J. Chem. Soc.*, *Dalton Trans.*, 1997, 129.

15 R. A. Leising, S. A. Kubow and K. J. Takeuchi, *Inorg. Chem.*, 1990, **29**, 4569.

16 F. Bottomley, H. Ekkehardt, J. Pickardt, H. Schumann, M. Mukiada and M. K. Kakihana, *J. Chem. Soc.*, *Dalton Trans.*, 1985, 2427.

17 J. B. Godwin and T. J. Meyer, *Inorg. Chem.*, 1971, **10**, 471.

18 R. A. Krause and K. Krause, *Inorg. Chem.*, 1982, **21**, 1714; S. Chakraborty, M. G. Walawalkar and G. K. Lahiri, *J. Chem. Soc.*, *Dalton Trans.*, 2000, 2875.

19 D. A. Bardwell, A. M. W. Cargill Thompson, J. C. Jeffery, J. A. McCleverty and M. D. Ward, *J. Chem. Soc.*, *Dalton Trans.*, 1996, 873.

20 L. M. Vogler and K. J. Brewer, *Inorg. Chem.*, 1996, **35**, 818.

21 G. A. Crosby and W. H. Elfring, Jr., *J. Phys. Chem.*, 1976, **80**, 2206.

22 R. Alsfasser and R. V. Eldik, *Inorg. Chem.*, 1996, **35**, 628.

23 K. D. Keerthi, B. K. Santra and G. K. Lahiri, *Polyhedron*, 1998, **17**, 1387.

24 B. K. Santra, M. Menon, C. K. Pal and G. K. Lahiri, *J. Chem. Soc.*, *Dalton Trans.*, 1997, 1387.

25 R. Samanta, P. Munshi, B. K. Santra, N. K. Lokanath, M. A. Sridhar, J. S. Prasad and G. K. Lahiri, *J. Organomet. Chem.*, 1999, **581**, 311.

26 R. P. Thummel and S. Chirayil, *Inorg. Chim. Acta*, 1988, **154**, 77.

27 W. R. Murphy, Jr., K. Takeuchi, M. H. Barley and T. J. Meyer, *Inorg. Chem.*, 1986, **25**, 1041.

28 A. K. Deb, P. C. Paul and S. Goswami, *J. Chem. Soc.*, *Dalton Trans.*, 1988, 2051.

29 V. R. L. Constantino, H. E. Toma, L. F. C. De Oliveira, F. N. Rein, R. C. Rocha and D. D. O. Silva, *J. Chem. Soc.*, *Dalton Trans.*, 1999, 1735; B. K. Ghosh and A. Chakravorty, *Coord. Chem. Rev.*, 1989, **95**, 239.

30 F. Bottomley and M. Mukiada, *J. Chem. Soc.*, *Dalton Trans.*, 1982, 1933; D. W. Pipes and T. J. Meyer, *J. Chem. Soc.*, *Dalton Trans.*, 1984, **23**, 2466.

31 J. E. Huheey, E. A. Keiter and R. L. Keitter, *Inorganic Chemistry*, Harper Collins College Publishers, New York, 4th edn., 1993, p. 650; T. A. Turney and G. A. Wright, *Chem. Rev.*, 1959, **59**, 497.

32 R. Samanta, P. Munshi, B. K. Santra and G. K. Lahiri, *Polyhedron*, 1999, **18**, 995; B. K. Santra and G. K. Lahiri, *J. Chem. Soc.*, *Dalton Trans.*, 1997, 1387.

33 T. B. Hedda and H. L. Bozec, *Inorg. Chim. Acta*, 1993, **204**, 103; G. B. Deacon, J. M. Patrick, B. W. Skelton, N. C. Thomas and A. H. White, *Aust. J. Chem.*, 1984, **37**, 929.

34 A. Bharath, B. K. Santra, P. Munshi and G. K. Lahiri, *J. Chem. Soc.*, *Dalton Trans.*, 1998, 2643.

35 B. M. Holligan, J. C. Jeffery, M. K. Norgett, E. Schatz and M. D. Ward, *J. Chem. Soc.*, *Dalton Trans.*, 1992, 3345; P. Munshi, R. Samanta and G. K. Lahiri, *J. Organomet. Chem.*, 1999, **586**, 176.

36 R. G. Wilkins, *The Study of Kinetics and Mechanism of Reactions of Transition Metal Complexes*, Allyn and Bacon, Boston, MA, 1974; R. Hariram, B. K. Santra and G. K. Lahiri, *J. Organomet. Chem.*, 1997, **540**, 155.

37 A. Pramanik, N. Bag, D. Ray, G. K. Lahiri and A. Chakravorty, *Inorg. Chem.*, 1991, **30**, 410.

38 B. K. Santra and G. K. Lahiri, *J. Chem. Soc.*, *Dalton Trans.*, 1998, 139.

39 D. T. Sawyer, A. Sobkowiak and J. L. Roberts, Jr., *Electrochemistry for Chemists*, 2nd edn., Wiley, New York, 1995.

40 G. M. Sheldrick, SHELXS 97, Program for crystal structure solution and refinement, University of Göttingen, 1997.